Paper Presented at the
11th Symposium of Thermophysical Properties, Boulder, Co. USA, June 1991

Isochoric Heat Capacity c_v at the Critical Point of SF_6 under Micro and Earth Gravity — Results of the German Spacelab Mission D1 —

J. Straub and K. Nitsche
Lehrstuhl A für Thermodynamik, Technical University
Arcisstr. 21, 8000 Munich 2, Germany

Keywords: Critical phenomena, isochoric heat capacity, critical relaxation, microgravity, D1–Mission

ABSTRACT

As a consequence of the diverging compressibility, earthbound experiments near the gas–liquid critical point suffer extremely from the strong influence of gravity. Caloric measurements, in particular of the heat capacity c_v, are inevitably affected by the local changes of density throughout the volume. Experimental results thus represent some integral average over all density and temperature variations rather than a thermodynamic point of state.

The first measurements of c_v under microgravity conditions for the fluid SF_6 near the critical state conducted during the German Spacelab Mission D1 in Oct./Nov. 1985 are reported here. Due to the surprising μg results, the influence of gravity and equilibration have been subsequently investigated. By numerical simulation of the equilibration process, it was clear that the flattening of the c_v curves observed was caused by a non–uniform mass distribution and the slow mass diffusion process.

INTRODUCTION

As the critical point of pure fluids is approached, the increasing sensitivity of the fluid to gravity causes problems in the measurements of critical phenomena on earth. Due to the high compressibility, earth gravity is sufficient to produce density stratification in experimental fluid cells, and the critical point itself thus appears only in a thin layer of the order of the correlation length at that given state. Even with the application of optical methods, the critical point itself evades observation because of the bending of the light beam due to the high corresponding refractive index gradient. In addition, the high value

of the thermal expansion coefficient results in a diverging Rayleigh number and makes the near critical system very sensitive to small temperature disturbances. It is for these reasons that critical point experiments have been among the first proposals to be conducted in the microgravity environment of the Space Shuttle, when this possibility was offered to scientists in the mid of 1970s.

In particular, studies that require a certain bulk fluid mass, e.g. in caloric measurements, suffer from the strong influence of gravity due to the height of the fluid sample, which can not be lowered beneath a finite value. As a result, we proposed in 1975 to develop a calorimeter and a High Precision Thermostat (HPT) to measure the heat capacity of a sample of pure fluid under microgravity conditions during a Spacelab Mission. The first laboratory equipment was developed and tested (Lange, 1984, Straub, 1986) and based on the collective experience a prototype, the so–called engineering module (EM) was constructed. After careful testing, an improved flight module (FM) was designed, and the calorimeter was in orbit within the German Spacelab Mission D1 in October 1985.

For the limited experimental time of about 100 h available at microgravity, a high resolution scanning ratio calorimeter seems to be the best design to measure the weak anomaly of the specific isochoric heat capacity. With the continuous electrical heating technique applied, small temperature ramps $\mathrm{d}T/\mathrm{d}t = \dot{T} = 3.6$ mK/h ≈ 1 K/11 days could be produced and within the 1 mm height of the specimen cell it was calculated that the thermodynamic equilibrium should be present despite the enhanced relaxation time close to the critical temperature. Even with a flat cell of only 1 mm in height, the influence of gravity could be observed, since the diverging compressibility generates the well known stratification. Thus, experimental c_v data in earth gravity below and above the critical temperature are dependent on the hydrostatic height and the temperature ramp, by which the theoretically predicted peak is flattened.

INFLUENCE OF GRAVITY ON A FLUID OF CRITICAL STATE

Since 1872, when van der Waals established his well–known equation of state, it is known that at the critical point the compressibility diverges, along with other thermodynamic properties. Those properties directly related to the compressibility cause the observed "anomalies" known as "critical phenomena". The isothermal compressibility is defined and written along the critical isochore as a power law:

$$\chi_T = \frac{1}{\varrho}\left(\frac{\partial \varrho}{\partial p}\right)_T = \frac{\Gamma}{p_c} \cdot \tau^{-\gamma} \qquad (1)$$

where $\tau = \frac{|T-T_c|}{T_c}$ is the temperature difference reduced to the critical temperature T_c, and γ is the critical exponent, with a value of 1.24 according to the Renormalisation Group Approach (RGA) and unity according to van der Waals and "classical" equations. Related to the compressibility is the isobaric thermal expansion coefficient and the isobaric specific heat.

A second group of properties are related to the isentropic coefficients and the isochoric heat capacity. Their divergency is weak, and therefore difficult to determine experimentally. However, there exists a special interest in theoretical considerations, e.g. the first theoretical solution of the two dimensional Ising model results in a diverging c_v, or in classical theories c_v is finite and according to RGA it follows a power law as:

$$c_v/R = A^{+,-} \cdot |\tau|^{-\alpha} + B \tag{2}$$

with the critical exponent $\alpha = 0.11$. The basic problem in experimental investigations here is caused again by the gravity field, due to the increasing compressibility which acts to compress the critical fluid under its own weight. This can be expressed by combining the hydrostatic pressure equation

$$\mathrm{d}p = -\varrho g \, \mathrm{d}z \qquad \text{with eq. (1)} \qquad \frac{\mathrm{d}\varrho}{\mathrm{d}z} = -\varrho^2 \cdot \vec{g} \chi_T \tag{3}$$

in an isothermal fluid, where z is the height variable in opposite direction of the gravity vector $\vec{g}$. It can be estimated that in a sample cell under gravity, the fluid at the critical state is compressed to a layer of the height of the correlation length. From critical opalescence it can be further estimated that this length is of the order of the wave length of light. Thus, even in a cell of 1 mm in height, only less than $1^0/_{00}$ of the total mass is actually at the critical state, and for a bulk mass measurement such as c_v, the result is the average due to the hydrostatic distribution and is not representative for measurements requiring a constant density path in accordance with the thermodynamic definition.

ISOCHORIC HEAT CAPACITY

The internal energy in terms of a unit mass of a pure substance and its total differential given as:

$$u = u(T, \varrho) \qquad \text{and} \qquad \mathrm{d}u = \left(\frac{\partial u}{\partial T}\right)_{\varrho} \mathrm{d}T + \left(\frac{\partial u}{\partial \varrho}\right)_{T} \mathrm{d}\varrho \tag{4}$$

$$\mathrm{d}u = c_v \, \mathrm{d}T - \frac{1}{\varrho^2}\left[T\left(\frac{\partial p}{\partial T}\right)_{\varrho} - p\right] \mathrm{d}\varrho$$

If the density in a system remains constant, c_v can easily be determined by its definition:

$$c_v = \left(\frac{\partial u}{\partial T}\right)_{\varrho} = \frac{\mathrm{d}u}{\mathrm{d}T} = \frac{\Delta u}{\Delta T} \tag{5}$$

where $\mathrm{d}u$ respectively Δu can be determined as the energy supplied to the system per unit mass, resulting in a temperature change ΔT. The second term in eq. (4) takes into account the local change of the density, which is the case in two–phase systems and critical systems, even if the average density remains constant.

A three dimensional plot of c_v close to the critical point is shown in Fig. 1, calculated from the Scaled–Equation of State (Albright, 1987) without the influence of gravity and relaxation effects. c_v follows the eq. (2) along the coexistence curve in the homogeneous liquid and vapor phase as well as along the critical isochore with various amplitudes $A^{+,-}$, while c_v is enhanced in the two–phase region by the phase transition energy and the increasing mass migration from liquid to vapor.

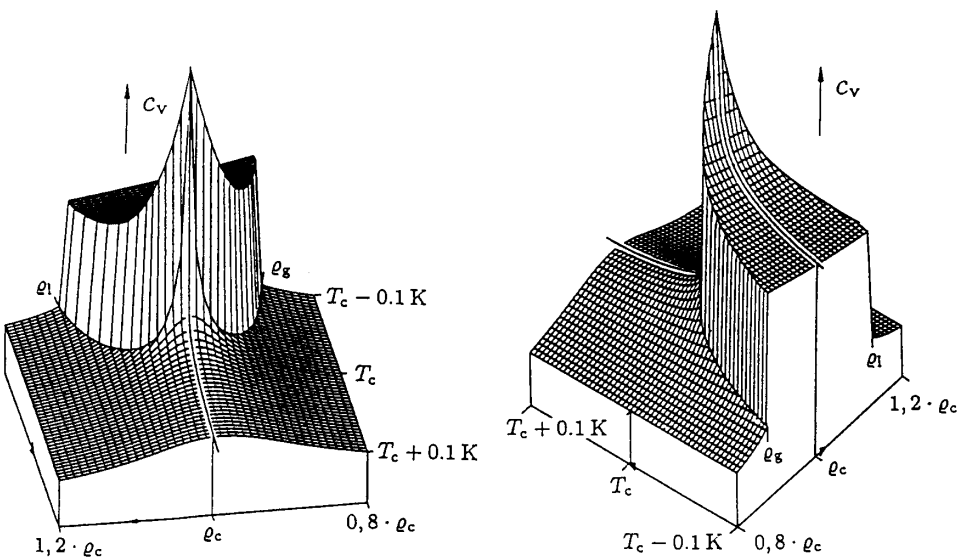

Fig. 1: Three dimensional plot of the isochoric heat capacity, calculated for CO_2, using the Scaled–Equation from Albright (1987)

In a compressible fluid, as is the case very close to the critical point, there exists even in equilibrium a density stratification for each temperature according to the compressibility and the hydrostatic pressure eq. (3). For a constant temperature at height level z, the specific internal energy is $u(z)$ and

the density $\varrho(z)$. The total energy of a cell of constant cross-section A and height H is the integral:

$$\overline{U} = A \int_0^H u(z) \cdot \varrho(z) \mathrm{d}z \tag{6}$$

Thus with a temperature change of the system, the internal energy changes with the local reorientation of the density as well. This must be taken into consideration in the heat capacity:

$$\bar{c}_\mathrm{v} = \frac{1}{H \cdot \bar{\varrho}} \int_0^H \frac{1}{\mathrm{d}T} \left(u\left(\varrho(z), T\right) \cdot \varrho(z)\right) \mathrm{d}z$$

$$\bar{c}_\mathrm{v} = \frac{1}{H \cdot \bar{\varrho}} \left[\int_0^H c_\mathrm{v}(z) \cdot \varrho(z) \mathrm{d}z + \int_0^H \left(\frac{\partial (u \cdot \varrho)}{\partial \varrho} \right)_\mathrm{T} \cdot \left(\frac{\partial \varrho}{\partial T} \right)_z \mathrm{d}z \right] \tag{7}$$

The first term is the average of the local capacities and the second term is the contribution of a local change of density with the temperature $(\partial \varrho / \partial T)_z$ at a constant height, given by:

$$\left(\frac{\partial \varrho}{\partial T} \right)_z = -\varrho p \beta_\varrho (\chi_T)_z \tag{8}$$

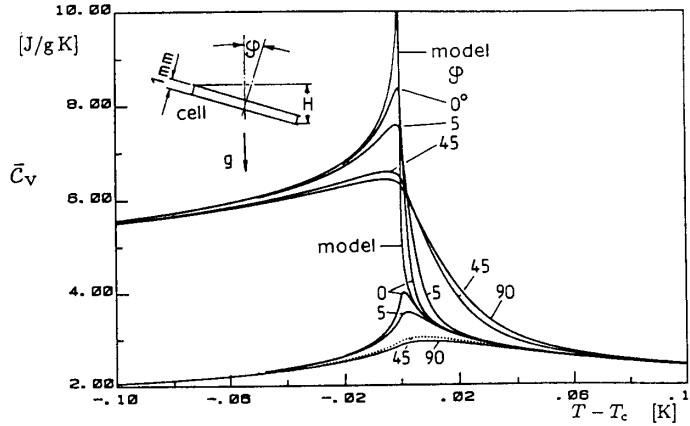

Fig. 2: Average heat capacity $\bar{c}_\mathrm{v}$, calculated for 1g condition and equilibrium, for CO_2 and for $\bar{\varrho} = \varrho_\mathrm{c}$. The lower band of the curves are the average values of local $\bar{c}_\mathrm{v}$ only.

For the equilibrium condition the evaluation of the integrals of eq. (7), using the Extended–Scaled–Equation from Albright (1987) for CO_2, is shown in Fig. 2 for the experimental cell used in this investigation, with 1 mm height and 30 mm in diameter. The cell is tilted from a horizontal position $\phi = 0°$ and 1 mm height to $\phi = 90°$ and 30 mm in height respectively, and the increasing flattening of $\bar{c}_v$ with increasing hydrostatic height is clearly visible. The lower band of curves are the integrals determined by the local capacities, the first integral of eq. (7). The difference between the corresponding curves is based on the density stratification, the second integral of eq. (7). It can also be seen that the temperature region influenced by gravity is within $(T - T_c) = \pm 0,1$ K.

MEASUREMENT METHOD

In order to use a calorimeter for measurements of c_v near the critical point and for the application during a Spacelab Mission with a limited experimental time, special emphasis is placed on the selection of the experimental method. In a cell of constant volume filled with a certain mass of the liquid under investigation, the average isochoric heat capacity can be measured in accordance with its definition.

The stepwise heating method is often successfully applied; however, close to the critical point c_v is a strong function of the temperature, and the temperature steps must be quite small, $\Delta T < 1$ mK, in order to produce a reasonable $c_v(T)$ function. For the required accuracy the resolution in the temperature measurement and the control of constant temperature after each step must be extremely high, of the order of μK. Moreover, it must be considered that a careful stepwise heating with the necessary equilibration time for a critical fluid between each step is a very time consuming procedure, not available at present during a Spacelab Mission.

Considering all the advantages and disadvantages of the various methods, the continuous heating method, called "scanning ratio calorimeter", was selected as the most suitable method for this special application purpose and successfully applied by Buckingham (1973), Edwards, (1968), Thoen (1978), Würz and Grubic (1980), Lange (1984), and Edwards (1984).

A sketch of the scanning ratio method is presented in Fig. 3. The sample cell 0 is surrounded by a reference cell 1, which is electrically heated with a constant temperature ramp $\dot{T} = \mathrm{d}T/\mathrm{d}t$. The sample cell 0 follows the reference cell 1, with the power P_0 controlled in such a way, that the temperature difference between stage 1 and 0, $T_0 - T_1 \approx 0$, is almost zero, as well as can be controlled. The energy balance applied to the cell yields the following equation:

$$C_0 \left(\frac{\mathrm{d}T_0}{\mathrm{d}t} \right) = P_0 + P_{T,0} + Q_{0,1} \tag{9}$$

and

$$C_0 = m_{\text{Fluid}} \cdot c_{\text{v,Fluid}} + C_{\text{Cell}} \tag{10}$$

where C_0 denotes the total capacity of the cell including the fluid capacity, $\frac{dT_0}{dt} = \dot{T}_0$ the temperature ramp of the cell 0, P_0 is the electrical heating power at the cell, $P_{T,0}$ the electrical power dissipated in the thermistor mounted on the cell, $Q_{0,1}$ is the heat leakage between the cell 0 and 1, calculated with the small remaining temperature difference. The shell 2 as a guard shield was controlled as $T_2 - T_1 \approx 0$. To minimize the heat leakage between all cells the entire calorimeter was evacuated up to 10^{-6} mbar.. Thus the heat leakage is provided only by radiation, by supporting polyamid threads (Kevlar®) with small thermal conductivity ($\lambda = 0,05\ \text{Wm}^{-1}\text{K}^{-1}$) and by the enameled copper wires (0,05 mm in diameter) for the electrical circuits. The radiation heat transfer is reduced between the cells by using a low emissivity gold coating. After the mission and various ground tests in the laboratory the fluid was removed from the cell, and the cell capacity C_{Cell} was determined in an otherwise unchanged arrangement. For more details see Lange (1984), Straub (1986) and Nitsche (1990).

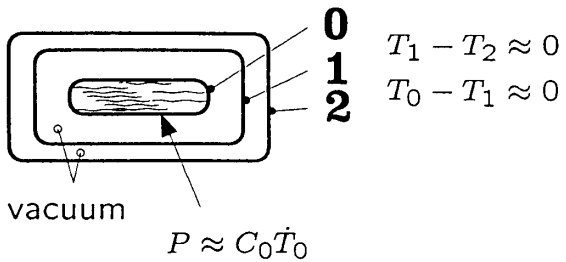

Fig. 3: Sketch of scanning ratio calorimeter

EXPERIMENTAL APPARATUS

Fluid Selection

The universal behavior of fluids near their critical point permits the selection of a fluid for this basic investigation which fulfills criteria necessary for a space mission: a reasonable critical temperature, a moderate critical pressure, critical data and region experimentally determined, a known equation of state, nontoxic and simple molecular structure. In the initial proposal $C0_2$ and Xenon were selected, since these substances have been well investigated before. However, Xenon, with a critical temperature of about 16 °C requires a cooling facility to operate a calorimeter around the T_c, and cooling with

peltier elements is more energy consuming than heating. The same holds true for $C0_2$ with $T_c = 31$ °C. At the time the development of the calorimeter was begun, it was not yet clear what the operational temperature in the Spacelab would finally be, 35 ° C as a maximum could not be excluded. Moreover, the critical pressure of CO_2 is high, at about 75 bar. Therefore sulfurhexafluorid SF_6 with 45,5 ° C as a critical temperature and a moderate pressure of 38 bar was selected instead. In addition, the molecular structure is spherical and unpolar, and the substance is stable and nontoxic. However, in the 1970s, thermodynamic data for SF_6 were scarce. This has now changed in the meantime, and SF_6 is well established as a standard substance for the study of critical phenomena in microgravity. The SF_6 used was of very high purity, of 99.993 % in the liquid phase, and was supplied by Matheson Gas Products.

The High Precision Thermostat

An assembly drawing of the scanning ratio calorimeter used is shown in Fig. 4.

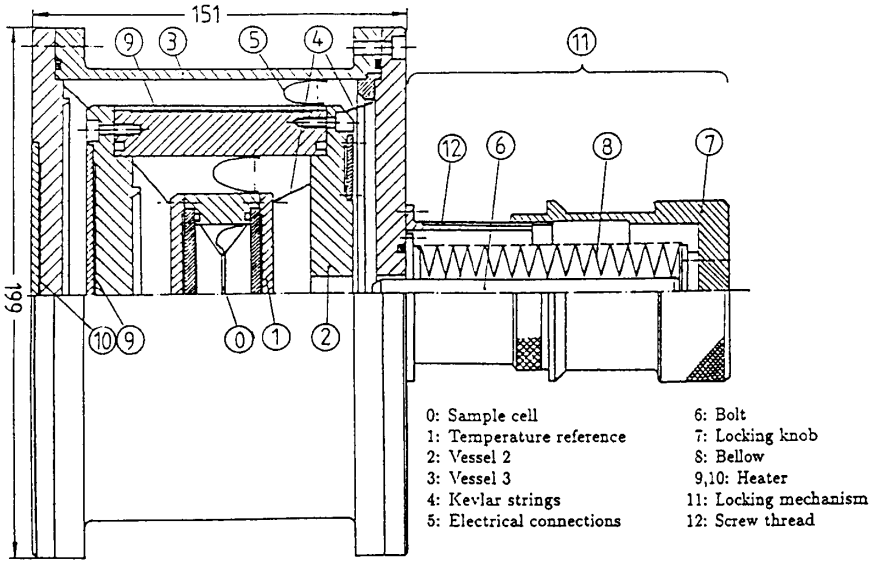

Fig. 4: Design of the calorimeter

It is described in greater detail in Lange (1984) and Straub (1986). The special construction imposed on a calorimeter operating in orbit was basically determined by the limited space and weight, limited electrical energy supply, and limited crew attendance as well as a mechanical resistance to withstand strong vibrations and high acceleration during launch and landing. Fig. 4 shows four concentric cylindrical vessels, 0 to 3. The coin–shaped sample cell 0, reference cell 1 and the adiabatic guard shield cell 2 are heated through

the critical temperature, applying constant power to stage 1, resulting in a constant temperature ramp. The electronic control system minimizes the temperature difference $T_0 - T_1$ and $T_1 - T_2$ by supplying electrical power to cell 0 and 2. To avoid damage during launch and landing cell 1 and 2 are pressed on the fixed cell 3 by a locking mechanism. The space tested hardware of the calorimeter within the highprecision thermostat outlined above was developed by Kayser–Threde, a Munich based space technology company.

The sample cell

The sample cell is the heart of the calorimeter, given in Fig. 5. The design is similar to the one used by Buckingham (1973), with a coin–shaped form of 1 mm height and 30 mm in diameter. The design fulfills three basic requirements:

- a low heat capacity of the stainless steel container,
- sufficient mechanical strength due to the high pressure fluid and
- a small hydrostatic height for terrestrial measurements.

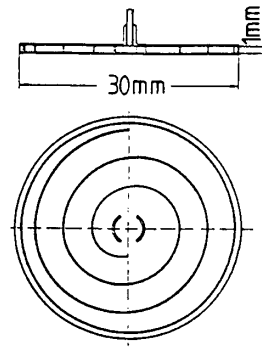

Fig. 5: Design of the sample cell

Inside the cell, a machined spiral mechanically supports the traverse flat sides soldered together, the spiral also acts as a fin to support thermal equilibration. With an interior height of less than 1 mm and heating on both flat sides, the thermal diffusion length is minimized. To reduce the capacity of the cell itself, the wall thickness was reduced to 0.2 mm. The fluid leakage through microcontraction cavities in the wall was avoided by using vacuum refined stainless steel. The cell was filled with SF_6 with the critical density; the correct mass was determined by a weighing procedure, according to the critical density $\varrho_c = 0.737$ g/cm^3. Taking into account the thermal and pressure expansion, the overall error of the filling of ± 0.5 % was calculated to be less than the uncertainty in the value of the critical density.

D1-MISSION IN 1985

The Spacelab Mission D1 was launched at Kennedy Space Center in October 1985. From the NASA Johnson Space Center in Houston, Texas, the experimental data were directly transferred to the German Mission Control Center of the DLR in Oberpfaffenhofen near Munich. Our laboratory computers were linked to the data network and permitted a quasi-real-time data evaluation, providing a means by which the astronauts could operate the apparatus manually as a contingency. This precaution was necessary for providing a successful experiment operation. During the mission three heating runs with different temperature ramps of 3.6, 10 and 100 mK/h within the gravity influenced window from $T - T_c = -100$ mK up to + 100 mK were planned. In order that the full mission time could be used for the calorimeter experiment, the HPT was scheduled to be the first experiment conducted during the orbit. However, problems with the vacuum system on the vent line created a delay of about 46 h, and later during the ramp, a servo loop imbalance required a readjustment of the electronic bridge by the astronauts. In addition, the first ramp was terminated early since the expected peak in the c_v curve could not be detected. As a result, the timeline was completely rearranged and thanks to the excellent cooperation of all groups involved, the scientists, the DLR and NASA operational managers and the astronauts, an additional ramp with 20 mK/h was able to be conducted within the 100 h available.

EXPERIMENTAL RESULTS

The first ramp running with 3.6 mK/h was the slowest. Therefore good equilibration even close to T_c and the best scientific results were expected. However, due to the readjustment of the thermistor bridge, data below T_c were lost and after missing the peak the ramp was aborted.

Together with the HPT data it was possible to record the gravity data. The large amount of data received both during and following the mission were carefully analysed, in order that all the information available be used. Simple averaging did not provide satisfactoring curves, and therefore a Fourier smoothing routine was implemented based on the virtual memory and as a result capable of smoothing "any" amount of data. The exact evaluation procedure is described in detail by Nitsche (1990) and will be published with more detailed results elsewhere.

In Fig. 6 the heat capacity $\bar{c}_v$ obtained in microgravity is compared with the power law eq. (2) and with experimental data for the 1 mm height cell under 1g-conditions with ramps of $\dot{T} = 1$ mK/h and 100 mK/h. The wiggly lines in

the μg runs clearly overlap the signal noise, and thus, maybe accepted as meaningful data. Due to the large thermal inertia in the c_v measurement, a direct interference due to gravity disturbances could not be detected. Regarding the wiggles and gravity disturbances, however, it could not be excluded that the mass distribution was correspondingly influenced by those, and thereby alters the mass diffusion length. The surprising results gave rise to careful discussions and examination of the apparatus. After the mission the HPT calorimeter was delivered as one unit to the author's lab in the original flight configuration. Without altering anything, the flight experiments were repeated under 1g–conditions.

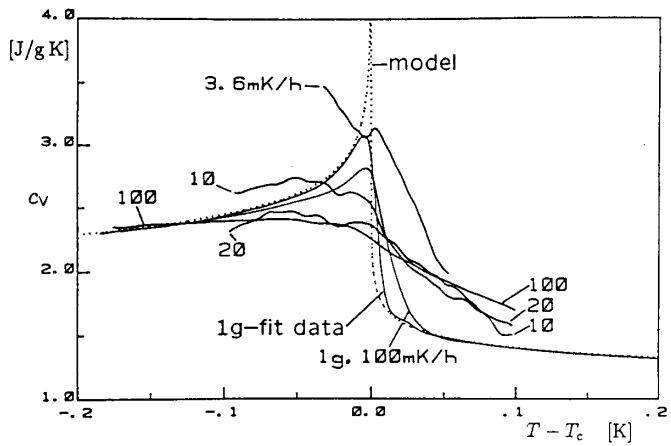

Fig. 6: $\bar{c}_v$–measured at microgravity during D1–Mission compared with measurements on earth at 1g

The critical peak and the $c_v(T)$ curves reappeared and proved the performance of the apparatus to be in proper working order as it was before the mission. The first apprehensions, that the cell filling had lost its critical density during the long period between delivery and the mission, were not confirmed.

During the first evaluations it was difficult to understand why equilibrium effects should cause this result, because the three different heating rates show a similar damped or flattened behavior of c_v. In addition, theoretical calculations for the experimental conditions yielded the result that at the most, only a few mK around T_c, could be influenced by a non established equilibrium. This is due to the fact that the cell is heated from both sides of the flat walls. The length, which must be considered as a characteristic length of equilibration, thus is half the cell height $H/2 = 0.5$ mm, or assuming a complete critical wetting of the cell walls, the length governing the equilibrium should be $H/4 = 0.25$ mm.

Measurements on earth

Careful measurements were conducted after the mission with the flight hardware in order to test the calorimeter, and to detect the primary causes of the effects that occur under microgravity. The normal heating run and some cooling runs were conducted, and additional stepwise heating and equilibration runs were performed. By tilting the entire thermostat from a horizontal position of the cell from $\phi = 0°$ and the height of 1 mm up to the vertical cell position $\phi = 90°$ and a height of 30 mm, the influence of various hydrostatic heights could be investigated. The results are shown in Fig. 7 with a constant temperature ramp of 100 mK/h. At one height $\phi = 0°$, however, various temperature ramps are shown in Fig. 8. If it is assumed that the temperature is to a large extent homogenized, then the c_v curve must be related to a delay in the density settling. It must be emphasized that, as mentioned before, both sides of the flat walls of the sample cell are heated; therefore, in all cases investigated, the length for the temperature equilibration is the same, $H/2 = 0.5$ mm. If convection enhances the equilibration, then the convection should even be higher at higher temperature ramps, and with a higher height the Rayleigh number as indication for the strength of convection increases with the third power:

$$Ra = \frac{g\alpha_p \Delta T \cdot H^3}{\nu \cdot D_{th}} \tag{11}$$

The delay in the equilibration should thus be reduced with higher ramps and at a higher cell height. It is of interest to note that a cooling ramp with

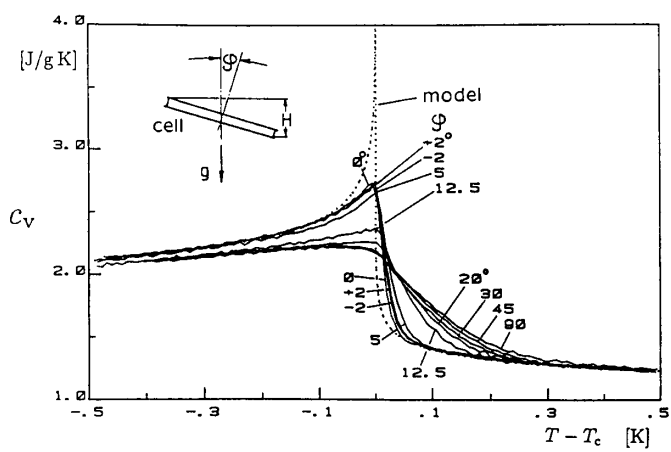

Fig. 7: Earth measurements of $\bar{c}_v$ at the same temperature ramp $\dot{T} = 100$ mK/h and various heights.

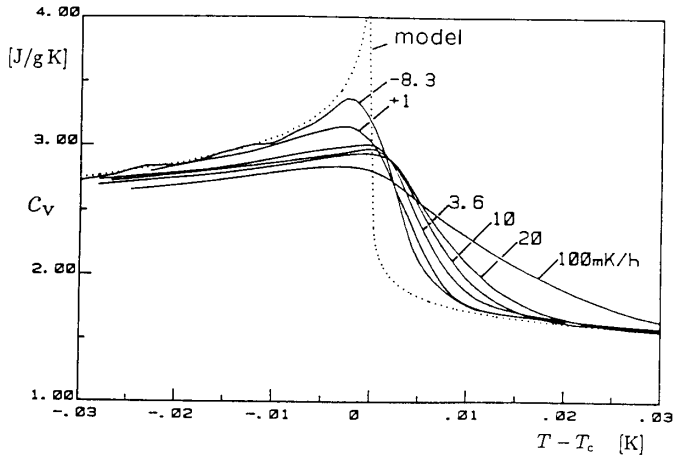

Fig. 8: $\bar{c}_V$ results for a constant cell height 1 mm and various temperature ramps.

8.3 mK/h and a ramp with 1 mK/h heating results in a c_v curve closer to the theoretical model. This supports the previous discussion: during cooling the experiment starts in the homogeneous density region, the density stratification is retarded, and even closer to T_c the density is more uniform than at the heating ramps coming only from the two-phase regions, with a complete separation of the liquid and vapor phase and at great difference between them.

A very careful analysis of all data confirms the asymptotic power law, eq. (2), in a temperature range $5 \cdot 10^{-5} < |\tau| < 1.6 \cdot 10^{-3}$ with $A^- = 15.81$, $A^+ = 8.135$, $\alpha = 0.1075 \pm 0.0005$, $B = 5.30$ and $A^-/A^+ = 1.943$. These values are in good agreement with other authors, e.g. Lange (1984), Edwards (1984) and RGA.

Relaxation Measurements

The Calorimeter can also be used in a stepwise heating mode. The sample cell was heated above the temperature of the cell 1 and kept at a constant temperature difference $T_{0,1} - T_1$ over approximately 3 hours. During this time the thermal coupling coefficient, which is the heat transfer coefficient times the surface area, could be determined from the power necessary to maintain the temperature difference and $P_{0,1} = K_{0,1}(T_{0,1} - T_1)$. After this the power to the sample cell was switched off and the cell equalized to the temperature of cell 1. The temperature difference between the cell 0 and cell 1 is an exponential function of time, $(T_0 - T_1) = f(t)$, by solving the energy equation for that case:

$$\frac{T_0 - T_1}{T_{0,1} - T_1} = exp(-t/\tau^*_{0,1}) \qquad \text{where} \qquad \tau^*_{0,1} = \frac{C_0}{K_{0,1}} \tag{12}$$

The time constant $\tau^*_{0,1}$ is directly related to the heat capacity C_0 of the cell, eq. (10). With the heat transfer coefficient $K_{0,1}$ the fluid capacity now can be determined. This stepwise heating and relaxation were carried out with small steps, of the order of mK, and within $|T - T_c| < 8$ mK with steps of 0.5 mK. Fig. 9 shows the resulting c_v data and the c_v curve according to the model. The data fit well the other curves, the scattering is larger, however, this is due to the small temperature steps. These results are in contrast to the findings of Dahl and Moldover (1972) and Edwards (1984) and others.

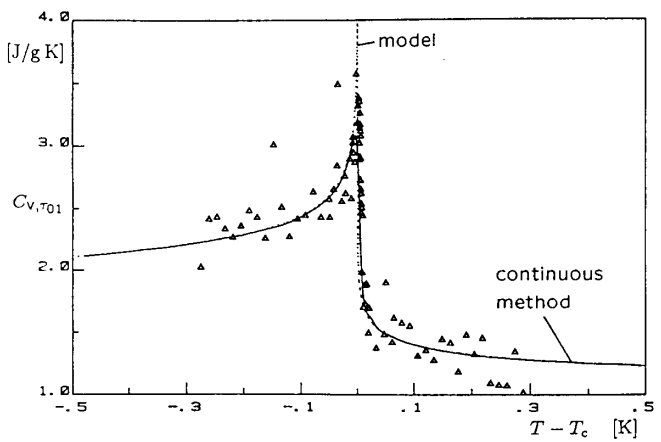

Fig. 9: $\bar{c}_v$ determined by thermal relaxation

EQUILIBRATION

The continuous heating applied with the scanning ratio technique generates permanent spatial temperature and density gradients in the sample cell. Therefore heating rates have been chosen that are moderate enough to render the inhomogeneities in the temperature and density field negligible. However, to establish this with rigor the equilibration process must be examined.

Experimental Observation

Observations made over many years of experimental studies of near critical systems are listed as follows:

- the temperature equilibration is fast,
- the density or mass equilibration is very slow.

The first statement was confirmed in a microgravity experiment carried out during a ballistic rocket flight TEXUS 8, Nitsche (1984). A cylindrical cell of 25 mm in diameter and 1.5 cm long was heated up, from $T - T_c = -0.4$ K to +0.4 K with a constant ramp within 6 minutes of microgravity. With a thermistor in the center of the cell and one at the wall, the thermal response was measured. On earth an almost constant temperature difference of 0.1 K between the center and the wall is maintained throughout the ramp. The heat transfer is enhanced by strong convection, as was observed through the cell windows at the flat cylinder faces. It can be seen in Fig. 10 that under microgravity the temperature in the center of the fluid follows the wall with nearly the same constant temperature difference as under earth conditions. Pictures taken from a 16 mm film show a conglomerate of liquid and vapor domains generated by the initial rocket spin. The clearly visible interfaces fade out as T exceeds T_c, and the inhomogeneous density field with local concentration and dilution domains remain until the end of the experiment at $T - T_c = 0.4$ K. This phenomena was also measured in a parallel cooling run with a second cell of the same design from $T - T_c = 0.4$ K down to $T - T_c = -0.4$ K. In this case the increasing turbidity in the cell was even over the area of the cell and completely opaque at T_c, and remained opaque over 3 minutes down to $T - T_c = -0.4$ K. Nearly the same temperature behavior was observed on earth, however, with strong convection, and phase separation.

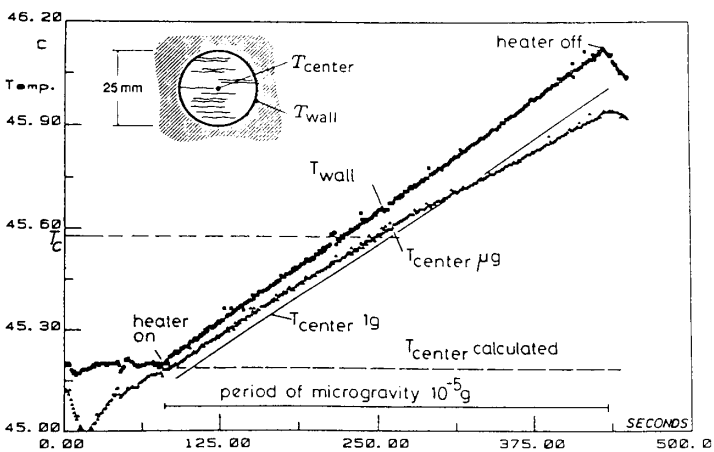

Fig. 10: Heating up a cell with critical density filling of SF_6 under microgravity TEXUS 8 from $T - T_c = -0.4$ K to + 0.4 K.

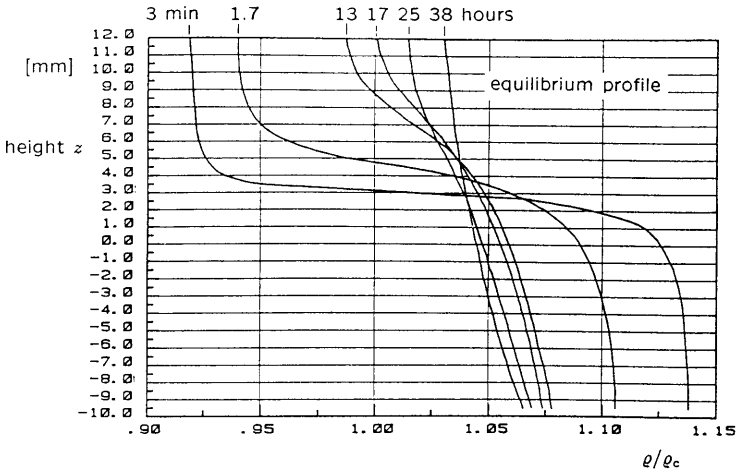

Fig. 11: Equilibration of density stratification profiles observed in N_2O at $T - T_c = 25$ mK after a disturbance by expansion and immediately compression. 38 h is the initial and final distribution.

These measurements and observations indicated that the temperature equilibration is fast even without convection, and that above T_c density inhomogeneities resulting from the two prior phases still exist above T_c.

In early measurements of density profiles (Straub, 1965) very slow density equilibrations have been observed; one example of this behavior is presented in Fig. 11. The system N_20 at supercritical temperature $T - T_c = 0.025$ K and average density $\overline{\varrho} = 1.04\ \varrho_c$ was expanded very fast to $\overline{\varrho} = 0.98\varrho_c$ and immediately thereafter compressed to its initial volume. Thus, the energy exhausted during the expansion was completely returned during the compression. The temperature of the cell was maintained. The initial equilibrium density profile returned after about 38 hours. The other profiles are taken after 3 min, 1.75, 13, 17 and 25 hours after the disturbance. This indicates that a fluid near a critical state is not at all completely elastic, or isentropic reversible, and that a density disturbed system requires a long period for equilibration.

Theoretical Approach

To describe equilibration or the equalization processes, the hydrodynamic equations for continuity, momentum and energy are applied to an elemental control volume. For a system of constant mass filled in a cell of constant volume, conservation of mass must be fulfilled. If we assume no gravity force, the velocities generated only by local volume change are very small, and the momentum equation can be neglected. The energy equation, can be derived

with the definition of the internal energy and the first law of thermodynamics, or with the entropy flow $\dot{S} = \dot{S}(T, \varrho) = \dot{S}(T, p)$, and the Fourier equation for the heat conduction:

$$\varrho c_v \frac{DT}{Dt} - \frac{T}{\varrho}\left(\frac{\partial p}{\partial T}\right)_\varrho \frac{D\varrho}{Dt} = -\nabla \dot{q} \tag{13}$$

where $\frac{D}{Dt}$ is the full differential.

With the definition of the heat capacity at constant pressure:

$$c_p = c_v - \frac{T}{\varrho_2}\left(\frac{\partial p}{\partial T}\right)_\varrho \left(\frac{\partial \varrho}{\partial T}\right)_p = c_v + \frac{T(p\beta_\varrho)^2}{\varrho}\chi_T \tag{14}$$

eq. (13) can be rewritten as:

$$\varrho c_p \frac{DT}{Dt} + \frac{T}{\varrho}\left(\frac{\partial \varrho}{\partial T}\right)_p \frac{Dp}{Dt} = -\nabla \dot{q} \tag{15}$$

The energy equation is usually applied in the last form. For systems of constant pressure, constant thermal conductivity and ignoring energy transport by convection, and using the Fourier law for heat conduction it follows the thermal diffusivity for constant pressure, which determines the time constant for such a system with characteristic dimension L:

$$D_{th} = \frac{\lambda}{\varrho \cdot c_p} \quad \text{and} \quad \tau^* = \frac{L^2}{D_{th}} \tag{16}$$

D_{th} goes to zero approaching T_c and the time constant for equilibration to infinity.

In the following the use of the energy equation according to eq. (13) is preferred, because both temperature and density changes are observable, and the density change is large, however, slow approaching T_c from the two-phase region. The first left term in eq. (13) is the energy necessary to equilibrate the temperature, the second is for the density equilibration and $\dot{q}$ is the total heat flux supplied to the volume element. This total heat flux can be separated into the two parts, which are necessary for the temperature and density change respectively the mass transport:

$$\dot{q} = \dot{q}_T + \dot{q}_m \tag{17}$$

Regarding the different time scales for temperature and density equilibration eq. (13) can be divided as:
for the temperature, respectivly the internal energy:

$$\varrho c_v \frac{DT}{Dt} = \nabla \lambda \nabla T|_T \tag{18}$$

and for the mass:

$$-\frac{T}{\varrho}\left(\frac{\partial p}{\partial T}\right)_\varrho \frac{D\varrho}{Dt} = \nabla \lambda \nabla T|_m \tag{19}$$

In eq. (19), the local temperature gradient necessary for the mass transport can be written as:

$$\nabla T|_m = \left(\frac{\partial T}{\partial p}\right)_\varrho \nabla p + \left(\frac{\partial T}{\partial \varrho}\right)_p \nabla \varrho \tag{20}$$

Assuming that at earth gravity in a later stage only a hydrostatic pressure gradient $\nabla p = -\varrho \cdot g$ exists in direction of the z–axis and convection terms are neglectible, the mass transport equation can be written for the z–direction (more generally the z-axis is normal to the interface):

$$\frac{\partial \varrho}{\partial t} = \frac{\partial}{\partial z}\left[\frac{\lambda}{T(p\beta_\varrho)^2 \chi_T}\left(\frac{\partial \varrho}{\partial z} + \varrho^2 \cdot g \chi_T\right)\right] \tag{21}$$

and with eq. (14)

$$\frac{\partial \varrho}{\partial t} = \frac{\partial}{\partial z}\left[\frac{\lambda}{\varrho(c_p - c_v)}\left(\frac{\partial \varrho}{\partial z} + \varrho^2 \cdot g \chi_T\right)\right] \tag{22}$$

This relation is the mass diffusion equation; the driving potential is the chemical potential, where $\varrho^2 g \chi_T$ is the density gradient or the chemical potential at earth gravity in the equilibrium case. The mass diffusivity from eq. 22 is:

$$D_m = \frac{\lambda}{\varrho \cdot c_v\left(\frac{c_p}{c_v} - 1\right)} = D_T \frac{1}{\left(\frac{c_p}{c_v} - 1\right)} \tag{23}$$

and the temperature diffusivity for constant density $D_T = \frac{\lambda}{\varrho \cdot c_v}$.

Close to the critical point

$$\left(\frac{c_p}{c_v} - 1\right) >> 1 \qquad \text{thus} \qquad D_m \approx D_{th} = D_0 \cdot \tau^\phi \tag{24}$$

the exponent ϕ is according to theory $\phi = \nu = 0.63$, the exponent of the correlation length, while in light scattering measurement experimental values

between 0.8 to 0.9 are obtained (Jany, 1987). For the critical isochore of SF_6: $D_0 = 0.2 \cdot 10^{-6}$ m/sec^2, $\phi = 0.83$. The exponent for

$$D_T = D_m \left(\frac{c_p}{c_v} - 1 \right) = D_m \left(\frac{\chi_T}{\chi_s} - 1 \right) \sim \tau^{\phi - \gamma + \alpha} \tag{25}$$

is $\phi - \gamma + \alpha$, and is between -0.5 to -0.3 depending on the value of ϕ. In any case, D_T is increasing approaching T_c, that means that the temperature equilibration is accelerated while the density equilibration is slowed down. The ratio of the time constants for mass diffusion τ_m^* and for temperature diffusion τ_T^* for the same characteristic length is as:

$$\frac{\tau_m^*}{\tau_T^*} = \frac{D_T}{D_m} = \frac{c_p}{c_v} - 1 \sim \tau^{-\gamma + \alpha} \tag{26}$$

τ_m^* represents the "critical slowing down" and τ_T^* the "critical speeding up".

Onuki (1989,1990) recently proposed a "piston model" with isentropic (adiabatic) heating of the bulk liquid, which was numerically confirmed by Boukari (1990) and Zappoli (1990). With this model the temperature equilibration is still faster than with the conduction model, however, it does not appear to be applicable to the two-phase system in regard to the interface, and at larger disturbances as long as $1/\chi_s \to 0$, with $\chi_s \sim c_v$, as the isentropic compressibility. The Onuki model can not replace the mass diffusion (eq. 22) necessary for two-phase systems and systems with density change at earth gravity.

For clarification it must be emphasized, that in case of a temperature change in the first step eq. (18) and (19) should be simultaniously solved. The density change at the wall induces a pressure change throughout the bulk volume, which results in the isentropic temperature change of the bulk, according to the piston model. Eq. (19) alone is used for the density equilibration in the late stage, for two-phase systems and remaining density inhomogeneities.

Analytical Approach

The solution of the differential equations (18) and (22) depends strongly on the initial and boundary conditions, and in the case of properties depending on temperature and density as it is close to T_c, these equations can only be solved numerically, as conducted by Nitsche (1990).

For the two-phase region it must be considered that, with the temperature the density change and a large amount of mass has to be transported from the liquid to the vapor phase. Assuming symmetric density between liquid and vapor phase, the liquid density and the density change is:

$$\frac{\varrho_l}{\varrho_c} = 1 + B \cdot |\tau|^{\beta} \tag{27}$$

differentiating yields:

$$\frac{\partial \varrho_l}{\partial T} = -\frac{\varrho_c}{T_c}\beta B \cdot |\tau|^{\beta-1} \quad , \qquad \text{where} \qquad \frac{\partial \varrho_g}{\partial T} = -\frac{\partial \varrho_l}{\partial T} \tag{28}$$

It should be recognized that near T_c, $\tau \rightarrow 0$, the mass flow rate crossing the phase interface is very high and finally diverges. The phase interface itself is not the "bottle neck" of the mass transport, as it was observed that the densities at the interface itself follows immediately according the temperature change (Straub, 1965). However, the mass transportation to the interface and from the interface into the vapor phase by diffusion is the mechanism which "slows down" the process.

If the fluid sample is heated or cooled with a constant temperature ramp, and no convection assumed at negligible gravity ($g \approx 0$), the temperature ramp can be expressed as a function of cell geometry, and the temperature difference ΔT permitted between the fluid center and wall. The maximum ramp to guarantee that ΔT is not exceeded is approximately:

$$\dot{T} = \frac{\Delta T}{L^2}\left(\frac{\lambda}{\varrho \cdot c_v}\right) 2(n+1) \sim \tau^{\phi-\gamma+\alpha} \tag{29}$$

where n = 0 is for plate with $L = H/2$ for a system heated from both sides, for cylinder n = 1, and for a sphere n = 2 with $L = R$. Eq. (29) is approximately valid for the temperature difference ΔT in the one phase and two–phase region (with $\dot{T} = 10$ mK/h, $T - T_c = 0.1$ K, $\Delta T \approx 2$ μK).

The mass equilibration up to $\Delta\varrho$ in the two–phase region, with $\Delta\varrho$ as density difference between the interface density and the bottom or top can be estimated as (attention $\Delta\varrho$ is not $\varrho_l - \varrho_g$):

$$\dot{T} = \frac{\Delta\varrho}{L^2} D_0 2(n+1) \frac{1}{\beta B} \frac{T_c}{\varrho_c} \cdot \tau^{\phi+1-\beta} \tag{30}$$

Eq. (30) is evaluated in Fig. 12. It can be seen in case of the flat cell that a diffusion length of $L = H/2 = 0.5$ mm, or with a complete wetting of the liquid $L = H/4 = 0.25$ mm, the ramp rates used should be adequate to balance the two phase region equilibrium reasonably.

INTERPRETATION OF THE MICROGRAVITY RESULTS

The fact that the calorimeter was in proper working order after the mission leads to the conclusion that the equilibration time was insufficient. With eq. (28) and the thermal diffusion length of $L = H/2 = 0.5$ mm, it can be calculated that the temperature difference ΔT between the center and

the wall is small enough to obtain good thermal conditions. In Fig. 12 it is seen that for the density equilibration, with a diffusion length of $H/2$, the ramp rates used should be adequate to achieve good equilibration conditions with $\Delta\varrho/\varrho_c = 0.01$ up to mK close to T_c. It was further expected that in microgravity, by complete wetting of the walls, the diffusion length for the mass should be reduced to $H/4 = 0.25$ mm, Fig. 13. This seems to be confirmed by a test during a NASA parabolic aircraft flight in the KC 135. A cell filled with SF_6 of critical density and at a temperature of about 1 K below T_c was used. It was observed that the liquid climbed up the cell walls and formed a vapor bubble in the center just at the point where gravity was reduced.

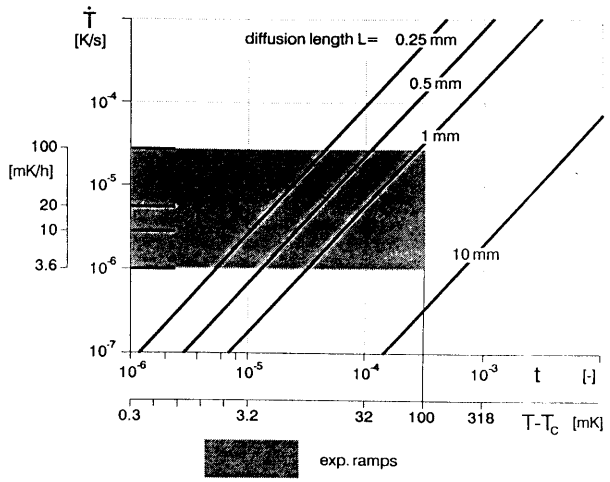

Fig. 12: Maximum temperature ramps for density equilibration up to $\Delta\varrho/\varrho_c = 0.01$ in the two phases below T_c

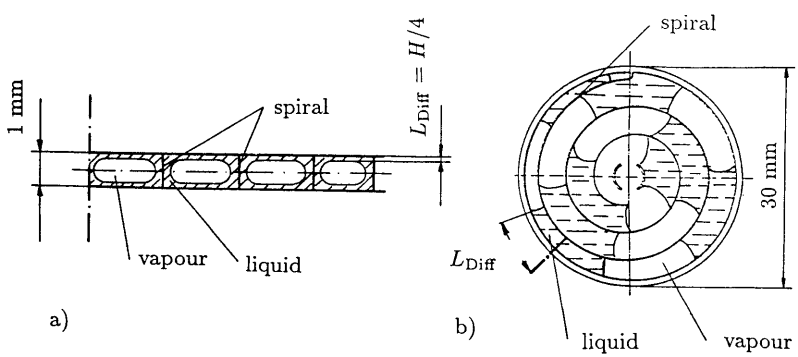

Fig. 13: a) Expected and b) possible mass distribution during microgravity

This wetting and the symmetric distribution of the liquid seems not to be the case in the calorimeter cell. It appears that the geometry and the spiral in the cell hindered the liquid from a regular distribution. Nitsche (1990) made a careful numerical calculation of the equilibration process and the resulting c_v curve. With the assumption of a diffusion length of 40 mm as initial liquid distribution for the first ramp of 3.6 mK/h and diffusion lengtb of 5 mm for the other ramps, c_v curves are received similar to the measured one, see Fig. 14. These calculations were conducted with the equation of state for CO_2 (Albright, 1987). CO_2 was used, because for SF_6 a reasonable equation of state was not available. For the mass diffusivity Fig. 11 was evaluated and a higher value determined as calculated with the equation (16) for the thermal diffusivity. Here a discrepance still exists, which has to be solved experimentally. With these considerations even the wiggles in the measured curves can be explained as caused by acceleration disturbances resulting in a change of the phase distribution with different diffusion lengths.

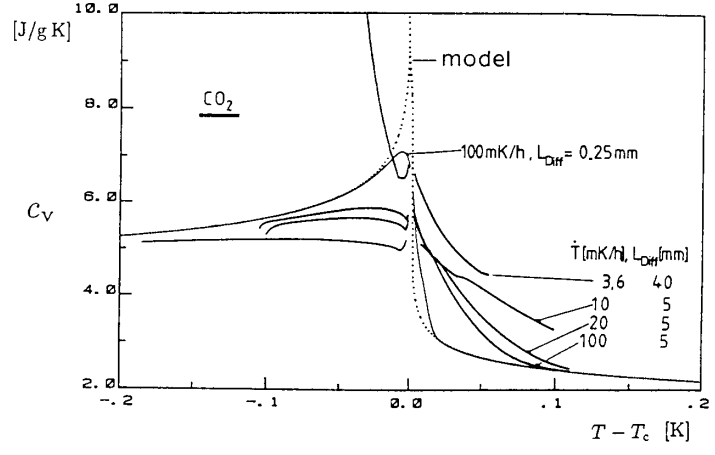

Fig. 14: Calculated $\bar{c}_v$–curves taking into account the mass diffusion and assumed diffusion length for CO_2

DISCUSSION

The critical point experiment conducted for the first time under a microgravity environment during a Spacelab flight led to unexpected, but nevertheless, interesting results. Initial interpretations of these results were greeted at first with scepticism, however, this opened up discussions concerning transient and nonequilibrium behavior of high compressible systems close to the critical point. It is now generally accepted that the temperature equilibration is

a fast process, either by our conduction model or the piston model proposed by Onuki (1989). The last one is applicable as long as the system reacts elastic and isentropic, which is the case for small pressure disturbances above T_c. The slow process near critical point is due to density equilibration and can be explained as a mass diffusion process driven by the difference in the chemical potential. This process can be regarded as the diffusion of clusters with various sizes which correspond to the correlation length. The correlation length itself depends on temperature and density. The mass diffusivity can be derived from the hydrodynamic energy equation and is in accordance with theory, however, it should be experimentally confirmed.

ACKNOWLEDGEMENTS

We gratefully acknowledge the financial support received from the Bundesministerium für Forschung und Technologie. We would also like to thank all individuals involved in the D1–Mission from NASA, DLR, the companies and the D1–Mission crew.

REFERENCES

Albright, P.C., Edwards, T.J., Chen, Z.Y., Sengers, J.V., (1987)
"A scaled fundamental equation for the thermodynamic properties of carbon dioxide in the critical region", J. Chem. Phys. **87**, No. 3, 1717 – 1725

Bloemen, E., Thoen, J., Van Dael, W., (1980)
"The specific heat anomaly in triethylamin–heavy water near the critical solution point", J. Chem. Phys. **73**, No. 9, 4628 – 4635

Boukari, H., Shaumeyer, J.N., Briggs, M.E., Gammon, R.W., (1990)
"Critical speeding up in pure fluids", Phys. Rev. A **41**, No. 4, 2260 – 2263

Buckingham, M.J., Edwards, C., Lipa, J.A., (1973)
"A high precision scanning ratio calorimeter for use near phase transitions", Rev. Sci. Instum. **44**, No. 9, 1167 – 1172

Dahl, D., Moldover, M.R., (1972)
"Thermal relaxation near the critical point", Phys. Rev. A **6**, No. 5, 1915 – 1920

Edwards, C., Lipa, J.A., Buckingham, M.J., (1968)
"Specific heat of xenon near the critical point", Phys. Rev. Lett. **20**, No. 10, 496 – 499

Edwards, T.J., (1984)
"Specific heat measurements near the critical point of carbon dioxide", Thesis, University of Western Australia

Jany, P., Straub, J., (1987)
"Thermal diffusivity of fluids in a broad region around the critical point", Int. J. Thermophys. **8**, No. 2, 165

Lange, R., Straub, J. (1984)
"Die isochore Wärmekapazität fluider Stoffe im kritischen Gebiet — Voruntersuchungen zu einem Spacelab Experiment", BMFT Forschungsbericht W 84-034

Lipa, J.A., Edwards, C., Buckingham, M.J., (1977)
"Specific heat of CO_2 near the critical point", Phys. Rev. A **15**, No 2. 778 - 789

Nitsche, K., Straub, J.. Lange, R., (1984)
"Ergebnisse des TEXUS-8-Experimentes Phasenumwandlung", Forschungsbericht Luft- und Raumfahrt, BMFT

Nitsche, K. (1990)
"Die isochore Wärmekapazität im kritischen Gebiet von SF_6 unter Erdschwere und reduzierter Schwere bei verzögertem Dichteausgleich", Thesis, Technical University, Munich (1990)

Onuki, A., (1989)
"Slow relaxation in microgravity and effects of stirring on critical point experiments", NASA. Workshop (1989) at NIST Gaithersbury

Onuki, A., Hao, H., Ferrell, R.A., (1990)
"Fast adiabatic equilibration in a single-component fluid near the liquid-vapour critical point", Phys. Rev. A **41**, No. 4, 2256 - 2259

Straub, J., (1965)
"Dichtemessungen am kritischen Punkt mit einer optischen Methode bei reinen Stoffen und Gemischen", Thesis, Technical University, Munich

Straub, J., Lange, R., Nitsche, K. and Kemmerle, K. (1986)
"Isocoric Specific Heat of SF_6 at the Critical Point: Laboratory Results and Outline of a Spacelab Experiment for the D1-Mission in 1985", Int. J. Thermophysics **7** (1986), pp 343 - 356

Thoen, J., Bloemen, E., Van Dael, W., (1978)
"Heat capacity of the binary liquid system triethylamin-water near the critical solution point", J. Chem. Phys. **68**, No. 2, 735 - 744

Würz, U., Grubic, M. , (1980)
"An adiabatic calorimeter of scanning ratio type", J. Phys. E: Sci. Instrum. **13**, 525 - 529

Zappoli, B., Bailly, D., Garrabos, Y., Le Neindre, B., Guenon, P., Beysens, D., (1990)
"Anomalous heat transport in supercritical fluids under zero gravity by the piston effect", Phys. Rev. A **41**, pp 2264